Desalination and Water Treatment
www.deswater.com
doi: 10.1080/19443994.2014.940638

55 (2015) 3267–3276
September

Taylor & Francis
Taylor & Francis Group

Experimental evaluation of a multiple-effect distillation unit in low seawater flow conditions

M.C. Georgiou[a,*], A.M. Bonanos[a], J.G. Georgiadis[a,b]

[a]*Energy Environment and Water Research Center, The Cyprus Institute, Nicosia 2121, Cyprus, Tel. +357 22 208 604; Fax: +357 22 208 625; email: m.c.georgiou@cyi.ac.cy*
[b]*Department of Mechanical Engineering, University of Illinois at Urbana-Champaign, Urbana, IL 61820, USA*

Received 9 April 2014; Accepted 16 June 2014

ABSTRACT

In this work, we evaluate experimentally the performance of a multiple-effect distillation (MED) unit in low seawater flow conditions and the potential of its integration with a concentrated solar power system. The innovation of this MED unit is the introduction of a flow distributor within the parallel plates of the falling film heat exchanger, designed to improve the system performance and efficiency under low seawater flow conditions. The main parameters examined were the thermal input power and the flow rate of the inlet seawater to each effect and the inlet seawater temperature of the single unit. Furthermore, the experimental results were compared with a control volume energy conservation model. The results showed that lower heat input load results to a higher value of the performance ratio (*PR*) of the unit and also under constant heat load, a higher temperature of the seawater lead to higher distillate product for the single effect unit. As the number of effects is increased the *PR* of the unit also increases approximately by 0.7 per effect. This maximum value for each effect is always observed in a constant ratio of seawater to steam flow rate.

Keywords: Multiple-effect distillation; Desalination; Solar thermal energy; Performance ratio; CSP

1. Introduction

Cyprus throughout its history has been facing several periods of water scarcity due to a combination of limited availability and excess demand of water [1]. According to the water exploitation index, an index that compares available water resources in a country with the amount of water used, Cyprus is considered to be water stressed. An index above 20% indicates water poverty for an EU country and Cyprus had an index above 40% in 2007 [2].

Furthermore, the observed and recorded climate change over the past few decades, especially in the Mediterranean region, is another significant factor contributing to the reduction of precipitation [3]. Many global and regional models predict a warming of several degrees in the Mediterranean by the end of the twenty-first century, with the warming in the summer being larger than the global average [4,5].

*Corresponding author.

Presented at the Conference on Desalination for the Environment: Clean Water and Energy 11–15 May 2014, Limassol, Cyprus

As a result of water scarcity, alternate means for obtaining freshwater, such as through seawater desalination [6], must be pursued. The increasing demand for freshwater due to population increase, coupled with the decreased rate of replenishment of the freshwater resources due to climate change impacts, necessitates the pursuit of desalination through renewable energy technologies [7,8].

A desalination process separates saline water into two parts—one that has a low concentration of salt (treated water or product water) and the other with a much higher concentration than the original feed water, usually referred to as brine concentrate or simply as brine. Commercially, the major types of technologies used for desalination can be divided in two types: thermal desalting technology and membrane desalting technology. Thermal desalting technologies include multi-stage flash distillation (MSF), multi-effect distillation (MED) and vapour compression, while membrane technology includes electro dialysis and reverse osmosis (RO).

As the name implies, thermal technologies involve the heating of saline water and collecting the condensed vapour (distillate) to produce pure water. The MED process has been used since the late 1950s and early 1960s and consists of several consecutive vessels (effects), maintained at decreasing levels of pressure (and temperature), leading from the first (hot) stage to the last one (cold) [9]. The main advantage of an MED unit compared with RO is lower electricity consumption due to the higher thermal input needs. Thus, the electrical energy for RO is about 3.5–4 kWh/m^3 while for MED unit is about 1–2 kWh/m^3. Compared with other thermal technologies such as MSF, MED has less total primary energy demands, lower power consumption and also has a higher performance ratio. Additionally, the usage of plate heat exchangers (PHE) resulted in higher heat transfer coefficients and also lower fouling resistances [10].

Each effect contains a multi-phase heat exchanger. Seawater is introduced in the evaporator side and heating steam in the condenser side. As the seawater flows down the evaporator surface, part of it is evaporated, while the remainder collects at the bottom of each effect as brine [11]. The pure water vapour raised by seawater evaporation at a lower temperature than the vapour in the condenser, due to the boiling point elevation observed in saline solutions. However, it can still be used as heating medium for the next effect where the process is repeated.

The decreasing pressure from one effect to the next one allows brine and distillate to be drawn to the next effect where they will flash and release additional amounts of vapour at the lower pressure [12]. This additional vapour will condense into distillate inside the next effect. In the last effect, the produced steam condenses on a heat exchanger, called distillate or final condenser and, which is cooled by the seawater used in the first effect.

The main drawback of all seawater desalination technologies, however, remains the high-energy consumption. In Cyprus, it has been estimated that the production of 1 million m^3/d fresh water requires 10 million tons of oil per year [13]. Due to high cost of conventional energy sources and considering the increasing trend in fossil fuel prices, renewable energy sources have gained more attention since their use in desalination plants will save convectional energy for other applications, reduce environmental pollution and provide free, renewable energy source [14].

As with any technology that generates power through prior heat generation, concentrated solar power (CSP) has scope for the application of co-generation. CSP plants can generate electricity which can subsequently be used for membrane desalination via RO, but they can also produce combined heat and power [15]. Thus, also thermal desalination methods like MED can be coupled to a CSP plant in an integrated co-generation scheme, as schematically depicted in Fig. 1. The thermodynamic integration of the electricity and desalination cycles, allows for increased efficiency to be achieved in both cycles, due to the larger fraction of useful energy extracted from each unit of thermal energy introduced to the system [16,17].

One application in which heat from CSP plants could be used is desalination, especially at a time when many regions, such as the Middle East and Northern Africa region, those are suitable for CSP due to their large levels of solar irradiation, face severe fresh water deficits. MED is more efficient than MSF in terms of primary energy and electricity consumption and has a lower cost. Moreover, the operating temperature of MED is lower, thus requiring steam at lower pressure if connected for combined generation to a steam cycle power plant. Thus, the combination of CSP with MED, as it is shown in Fig. 1, will be more effective than a combination of CSP and MSF desalination.

In the present paper, a three-effect distillation (MED) unit for seawater desalination was constructed in order to experimentally characterize its performance when operating under variable thermal load or under variable seawater feed flow rates. This allows the optimal operating conditions to be determined, particularly under low-flow conditions. A one-dimensional theoretical model to predict the performance of the device is developed and validated against the experimental results obtained.

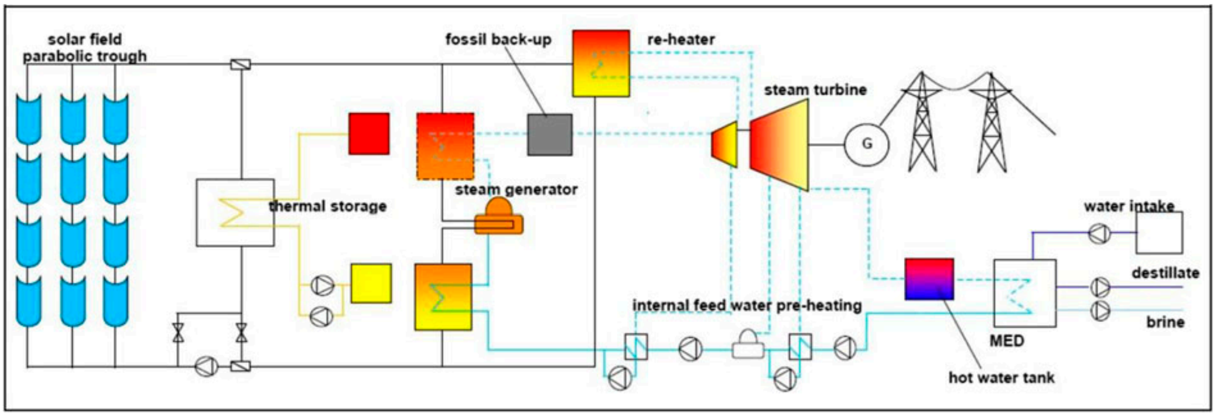

Fig. 1. Multiple effect desalination using heat and power from a CSP plant [18].

2. Experimental procedure—data analysis

2.1. Experimental set-up

A three-effect MED unit with a forward feed water configuration, as shown in Fig. 2, was constructed to evaluate the performance of a small-scale MED unit under low-flow operating conditions. The key components of the experimental set-up are the effect vessel, the multi-phase heat exchanger, the final condenser, the vacuum pump and the peristaltic pumps for extracting brine and distillate product. In order to minimize thermal losses to the environment, the effects were thermally insulated.

The present implementation utilizes PHE as a more compact and efficient way to transfer heat from the steam to the seawater, as opposed to the traditionally used shell-and-tube heat exchangers [19]. The steam will pass through the plates of the heat exchanger, condense and return back to the boiler, while the saline water boils and thus evaporates. The water vapour is ported to the final condenser, in which it is cooled down by passing cold water through the heat exchanger and it condenses into the distillate product.

To ensure that the heat released from the heating steam will be transferred to the saline water, the condensation temperature of steam has to be higher than the boiling temperature of the saline water. To achieve this, the saline water boiling point is reduced by decreasing the pressure in the evaporator tank by a vacuum pump. The remaining brine water is removed

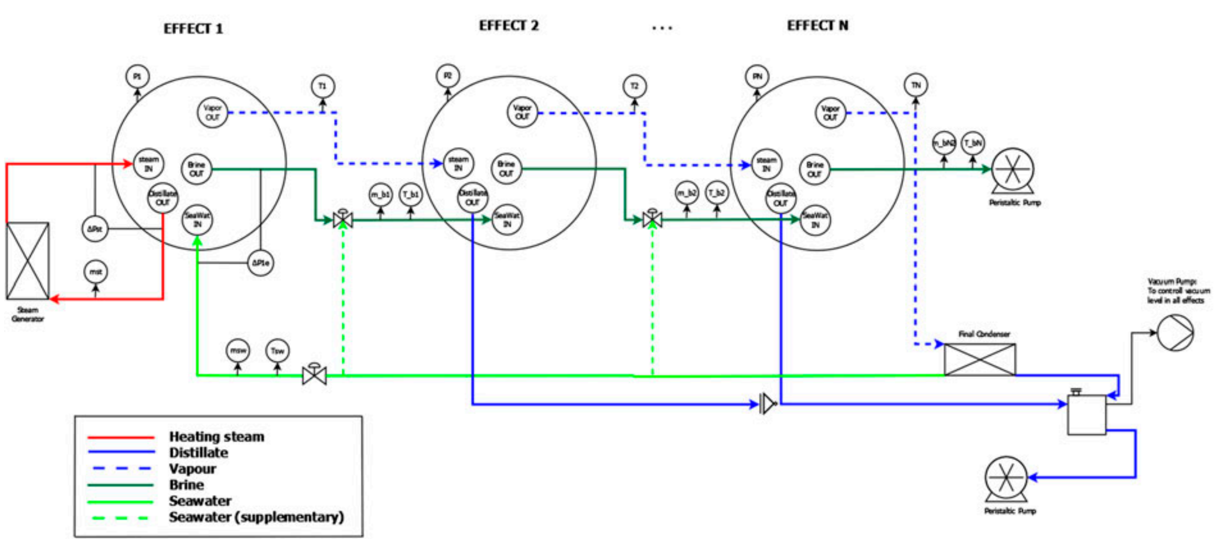

Fig. 2. Schematic of the three-effect distillation unit. Each circle represents the effect vessel and the input and outputs of each effect are indicated.

from the evaporator tank continuously via a peristaltic pump.

Since low-flow conditions were investigated, a critical challenge we had to face was the complete wetting of the heat exchanger plates, since it determines the heat transfer within the heat exchanger and thus the operational efficiency. During initial testing, it was observed that the plates were not all wetted; therefore, a flow distributor was designed and tested in order to better distribute the seawater flow over the heat exchanger. Several distributor configurations were experimentally evaluated, and a configuration with four holes, each 3 mm in diameter and spaced 8.5 mm apart achieved the greatest wetting on the heat exchanger plates [20].

2.2. Data acquisition and analysis

The experimental process was as follows: initially, the effects were evacuated to remove all non-condensable gasses and then steam and seawater were allowed to flow. The start-up process lasted about one hour, during which time the temperature of the system was gradually raised. Once a steady state was obtained, data acquisition commenced. A typical run lasted between 20 and 30 min and consisted of recording effect temperatures, pressures, flow rates and brine height level within the vessel. Temperatures were recorded using type-K thermocouples that were previously calibrated against a NIST traceable standard using an ice-point reference and an immersion heater, to reduce their error to ±0.4°C in the 30–150°C range. Subsequently, the parameter under investigation was varied and the process was repeated.

The aim during each run was to minimize the variation in flow properties and achieve a steady production of distillate. A statistical analysis was performed over all data samples gathered for a given run, and the variance and error were computed. The error bars correspond to an error propagation analysis. A 95% confidence interval was used reflecting a significance level of 0.05.

The steam generator employed had a cyclical variation in its output flow rate, attributed to its temperature controller. This lead to a fairly large variance in m_{st} and thus, large variances in all related quantities. Sample data from the flow meters are presented in Fig. 3, where the variation in m_{st} can be clearly seen, whereas in contrast, the seawater (m_{sw}) and brine (m_b) flow rates are fairly steady. The fact that the steam flow rate variation does not affect the operation of the effect is an indication of the robustness of the MED process.

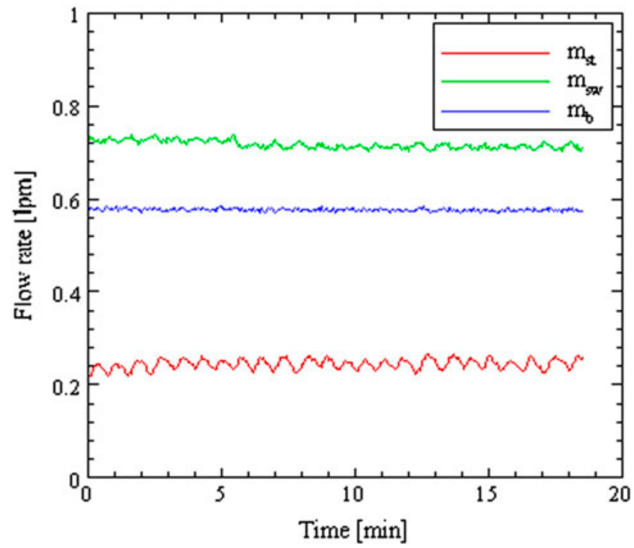

Fig. 3. Representative time record of flow meter sensor outputs collected from the single-effect MED.

2.3. Test matrix

Measurements were made in order to characterize the performance of the MED unit. The variation of the observed steam flow rate was taken into account in the data analysis. The steam generator was set at four different thermal power output levels ($Q_{e,1} < Q_{e,2} < Q_{e,3} < Q_{e,4}$) and measurements were repeated for each input load. The device performance is measured by computing the *PR*, a metric for the efficiency of thermal distillation systems defined as the ratio between the distillate and steam flows fed to the evaporator. The range of parameters investigated is summarized in Table 1.

3. Experimental results

3.1. Single-effect distillation unit

Complete wetting of the heat exchanger plates is critical for efficient operation of the heat exchanger

Table 1
Range of parameters varied in experimental studies

Parameter	Units	Range
$Q_{e,1}$	[kW_{th}]	4.2 ± 0.2
$Q_{e,2}$	[kW_{th}]	5.7 ± 0.3
$Q_{e,3}$	[kW_{th}]	7.6 ± 0.4
$Q_{e,4}$	[kWth]	8.8 ± 0.6
m_{sw}	[lpm]	0.20–0.72
$T_{sw,1}$	[°C]	19–22
$T_{sw,2}$	[°C]	30–32

itself, and by extension of the MED unit [21]. During initial testing, it was observed that the plates were not all wetted, due to low seawater flow rates. This was asserted by observing the outflow of the heat exchanger, where the flow exits only from the first 2–3 plates of the heat exchanger.

To remedy this situation, a flow distributor was constructed in order to better distribute the seawater flow over the heat exchanger. Several distributor configurations were experimentally evaluated, varying the hole size and spacing. A configuration with four holes, each 3 mm in diameter and spaced 8.5 mm apart achieved the greatest wetting on the heat exchanger plates as indicated by water exiting the heat exchanger throughout its thickness, and was therefore chosen.

In Fig. 4, the two curves represent the data collected on the single effect unit, with and without distributor for constant heat input conditions ($Q_{e,2}$). Whilst both curves have a maximum *PR* value for the same value of seawater to steam flow rate, an increase in *PR* by approximately 15% is achieved in the case with the flow distributor. Furthermore, the slope of the curve after the maximum value is smoother for the case with the distributor while without the distributor the *PR* value decreases more rapidly for higher seawater to steam flow rates.

An important conclusion from the distributor study is that the wetting of the heat exchanger plates is an important parameter affecting the performance of the unit at high seawater flow rates. Therefore, all the measurements for the single effect and all the additional effects will be done with the usage of flow distributors within the parallel plates.

The performance ratio obtained by varying the seawater flow rate for a given thermal input ($Q_{e,1}$) is presented in Fig. 5. The seawater flow rate is non-dimensionalized by the steam flow rate in order to aid comparison between the various cases of thermal input. The error bars represent the compounded uncertainty in the measurements due to each probe's error. It is important to note that the line connecting the experimental points is a curve-fit meant to aid the reader in visualizing the data, therefore, the maximum *PR* in the experimental points and the curve-fit might not be at exactly the same point. The same is true for the remaining figures of this text.

A maximum *PR* is observed for a normalized seawater flow rate of 1.7. When m_{sw} is decreased, there is not sufficient wetting of the heat exchanger plates, and so dry spots occur, leading to a decrease in the overall heat transfer coefficient and hence, a decrease in the performance of the device. On the other hand, when m_{sw} is increased, a larger fraction of the available thermal energy is required for elevating the feed temperature to the boiling temperature, and so less energy is available for the phase change process, leading to less distillate production and a lower *PR*.

The same trends as those observed in Fig. 5 for $Q_{e,1}$ input conditions are present for all thermal input conditions, as summarized in Fig. 6. Here, the error bars are omitted for clarity of the figure, but the magnitude of the error is similar to that presented in Fig. 6. For all thermal inputs, the maximum *PR* ratio measured remains almost constant at 0.71. Small variations in the magnitude of the *PR* are attributed to different seawater feed temperatures, as discussed below. As the thermal input to the system is increased, the

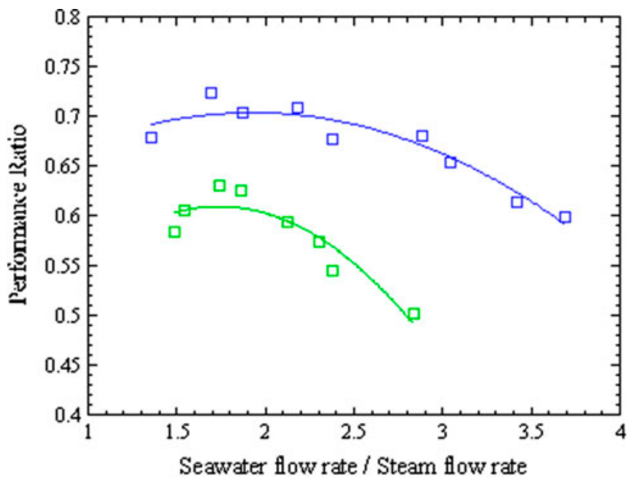

Fig. 4. Results for the single effect under a constant heat input ($Q_{e,2}$) with and without the distributor.

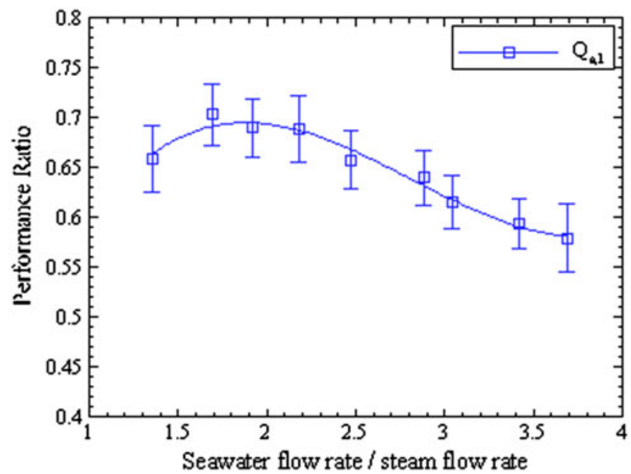

Fig. 5. Summary of results for single-effect distillation for a constant heat input ($Q_{e,1}$).

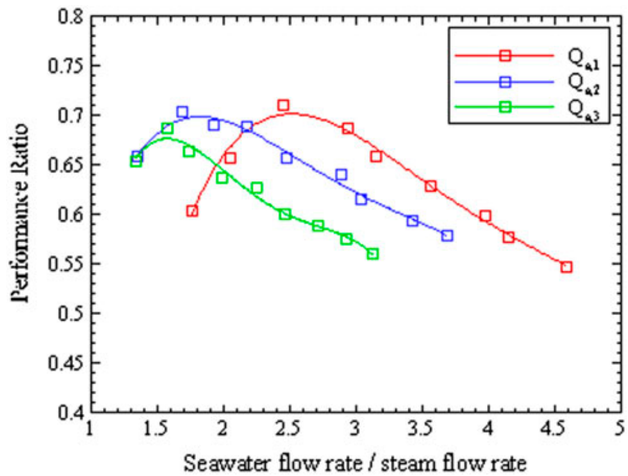

Fig. 6. Single-effect performance ratio results for three heat input conditions ($Q_{e,1}$, $Q_{e,2}$ and $Q_{e,3}$).

maximum *PR* shifts to the left, e.g. to a lower seawater flow rate, as more thermal energy is available for the same quantity of seawater and thus, evaporation and dry out will occur at lower flow rates.

Another parameter monitored was the temperature of the feed seawater. In a typical MED set-up, the seawater would be preheated since it would be used as the cooling fluid in the final condenser. However, in the present set-up, the seawater was not preheated and was drawn from a tank at ambient temperature. In order to outline the importance of the feed seawater temperature, the *PR* of the unit is given in Fig. 7 for the $Q_{e,2}$ thermal input condition and for two different seawater feed temperatures. The seawater feed temperature mainly depended on the outdoor conditions and the season of the experiments. The experiments presented herein were performed at two different ambient conditions, nominally $T_{sw,1} = 21\,^{\circ}\mathrm{C}$ and $T_{sw,2} = 31\,^{\circ}\mathrm{C}$. The shape of the two curves and the location of the maximum *PR* are similar. However, for $T_{sw,2} > T_{sw,1}$, higher *PR*s are obtained, as, again, less thermal energy is required for the preheating of the seawater and thus more energy is available for the production of distillate.

3.2. Two-effect distillation unit

The next step after the characterization of the single-effect distillation unit was the further expansion of the system to more effects. Thus, a second vessel was added in the system in a forward-feed configuration. In the forward-feed configuration, the direction of heat flow as well as the flow direction of the brine and vapour is from left to right, i.e. from effect 1 to effect *n*. The pressure in the effects decreases in the flow direction. The experimental procedure followed was the same as the single-effect unit. For a given thermal input (Q_e) and varying seawater flow rate, the *PR* of the unit was calculated.

The data collected for the two-effect unit are summarized in Fig. 8. Compared with the single effect results shown in Fig. 7 several conclusions emerge. First, there is a restriction to the maximum seawater flow rate that can be introduced into the system, due to a limitation in the experimental set-up and the flow rate that can be extracted by the peristaltic pump. Consequently, the curve is linear whilst it was expected to have a maximum value and then start decreasing as with the single-effect data. Additionally,

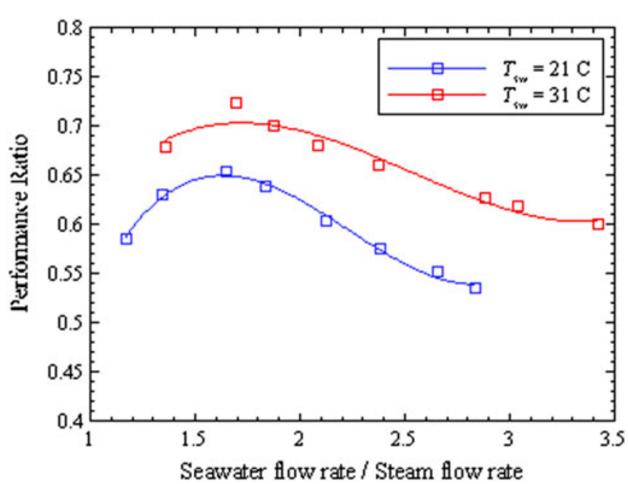

Fig. 7. Performance ratio curve under different seawater feed temperatures for constant heat input load ($Q_{e,2}$).

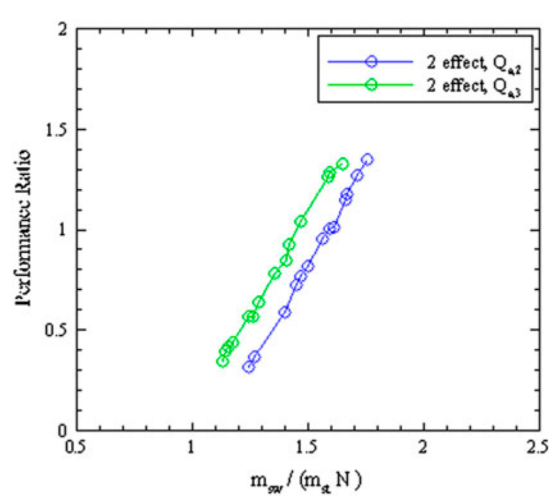

Fig. 8. Two-effect performance ratio for three heat input conditions ($Q_{e,1}$, $Q_{e,2}$ and $Q_{e,3}$).

the system cannot function under the lower heat input condition ($Q_{e,1}$) thus, data for only two curves are shown. Similar to the single effect, as the thermal input to the system increases the maximum of the *PR* of the system is decreasing as expected.

3.3. Three-effect distillation unit

Finally, a third effect was added to the system in the same forward-feed configuration. The data collected during the testing of the three effect distillation unit that are presented in Fig. 9. A similar behaviour to the single- and two-effect units is found. The maximum *PR* value is once again observed for the same seawater to steam flow rate value (approximately 1.7) as in the previous two cases. Due to the experimental modification, we managed to collect data for higher seawater rates and we concluded that the *PR* of the unit starts to decrease after the maximum *PR* value as it was observed in the single-effect unit.

3.4. Comparison of single-, two- and three-effect distillation unit

The best way to compare the experimental data obtained for single-, two-effect and three-effect distillation unit is to plot all the data together and identify the similarities or contraries that are observed. Thus, in Fig. 10, we have plotted the *PR* of each case as a function of seawater to steam flow rate for the same heat input conditions ($Q_{e,3}$).

All three curves have a maximum *PR* value at the same value for seawater to steam flow rate ratio (1.7) and the *PR* value is approximately the double for the two-effect units compared with the single effect and has a triple value for the three-effect unit compared with the single one. Despite the fact that the curve observed for the two-effect unit is debatable due to the absence of experimental points for higher seawater flows, the fact that the last point is identified at the same value for all three cases, strengthens our belief that this is the maximum of the curve and that for higher value of seawater to steam flow rate the *PR* will start decreasing.

Another point that is worth mentioned is the maximum value of the *PR* and the value of the seawater flow rate to steam flow rate. The *PR* in this figure has a maximum approximately at 2.2 for seawater to steam flow rate at 1.7 identifying that this maximum has the triple value of the maximum price obtained at the first effect for the same ratio of seawater to steam flow rate. Thus, we speculate that the seawater to steam flow rate value of 1.7 is the crucial point where the curve was expected to have the maximum of unit's performance and then start decreasing.

Lastly, via our experimental results, we assume that the shape of the curve is also modified especially after the crucial point. More precise in the first effect,

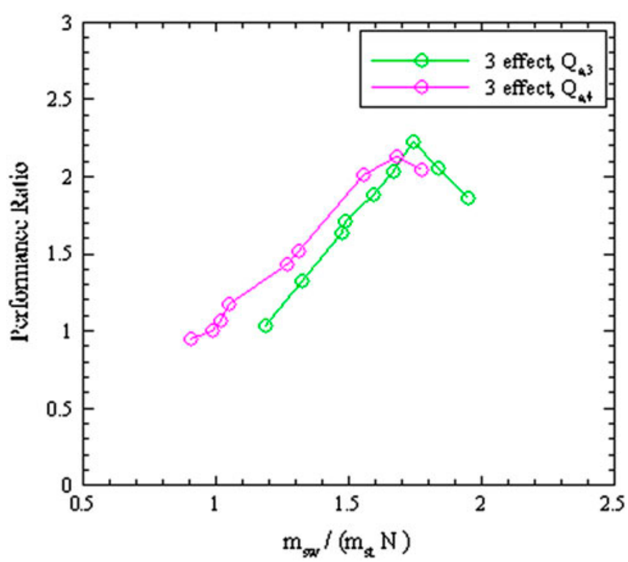

Fig. 9. Summary of results for three-effects performance ratio for all three different heat input conditions ($Q_{e,2}$, $Q_{e,3}$ and $Q_{e,4}$).

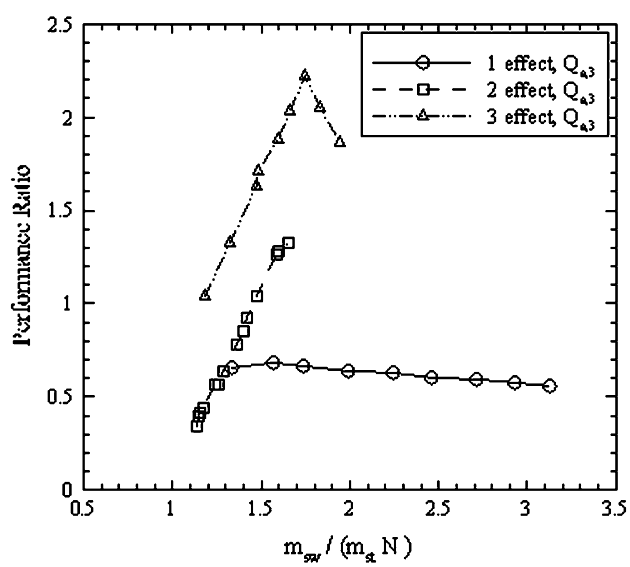

Fig. 10. Summary of results for single-, two- and three-effects performance ratio for constant heat input load ($Q_{e,3}$).

the *PR* value is smoothly decreased as we increased the seawater flow rate in values higher than the crucial point while in the three effects, the *PR* value is significant decreased for seawater flow rates higher that the ones corresponding to the maximum. Due to the limitation of the data-sets for the three effects this assumption is debatable but we anticipate that the results gained for the four-effect distillation unit will give a more clear indication.

4. Control volume model

In the literature, there are many theoretical models used for calculating the *PR* of a MED unit. There are models for forward-feed configuration, parallel-feed configuration and backward-feed configuration. One of these models, by Vozar et al., was used for evaluating the experimental results collected during our experiments.

This mathematical model is developed to analyse the system operating characteristics and the effect of various design parameters. The model is essentially a mass and energy balance and follows similar models in the literature [22,23]. The major model assumptions are steady-state operating conditions, zero salinity for the product water and that no non-condensable gases are present in the system.

The experimental conditions were used as input parameter to the model, which in turn calculated the *PR* and various other intermediate parameters in the effects. The results predicted from the models were compared with those evaluate in the MED set-up, as presented in Fig. 11. As expected, the models capture the decreasing trend in *PR* experienced as the seawater flow rate increases. However, the models are unable to capture the dry out occurring at low-flow conditions and thus are unable to predict the maximum in *PR*.

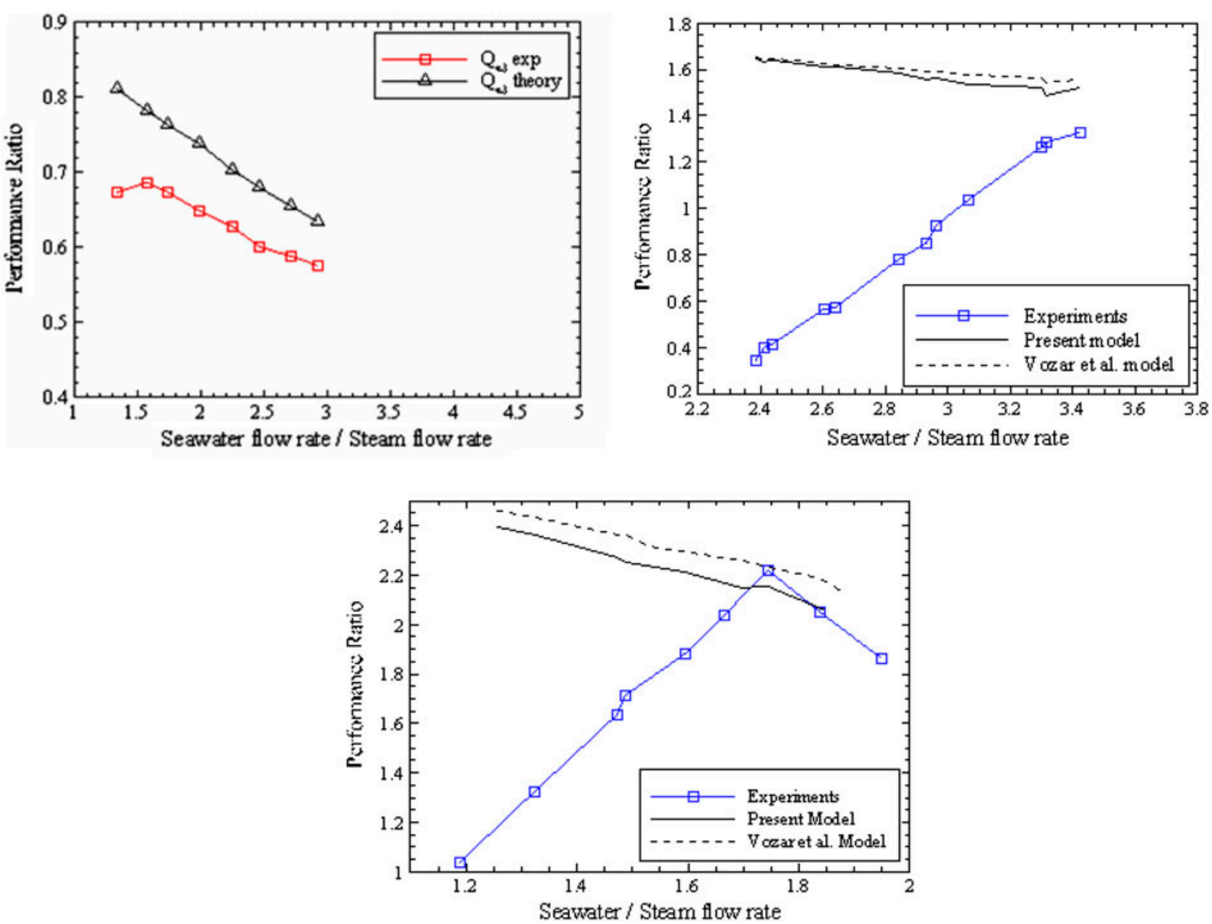

Fig. 11. Summary of results for single-, two- and three-effects performance ratio for constant heat input load ($Q_{e,3}$) compared with the theoretical results predicted by Vozar et al. [11] model and single-effect model.

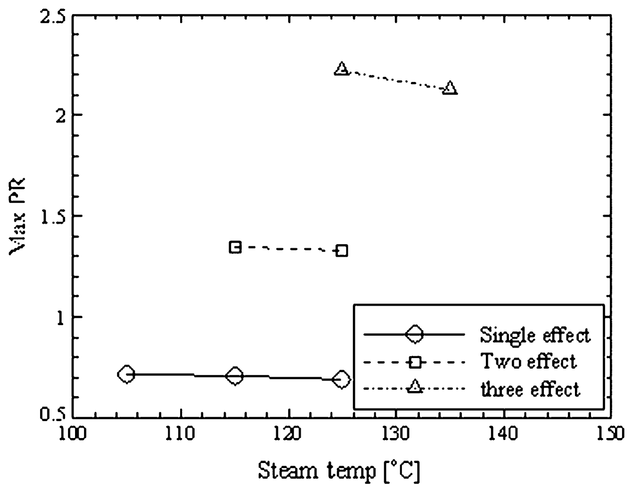

Fig. 12. Summary of results for single-, two- and three-effects performance ratio as a function of the heating steam temperature.

Additionally, Fig. 12 shows the *PR* of the unit as a function of the heat input steam temperature and the number of effects. As it is recorded in the literature [24,25] and showed through our experimental results also as the heating steam temperature and the number of effects increase the thermal performance of the system is decreased. This is caused by three factors:

- Increase in the amount of sensible heat required for increasing the temperature of the feed water to higher boiling temperatures since the feed temperature is kept constant.
- Increase in the amount of feed flow rate.
- Decrease in the latent heat of the heating steam at higher temperatures.

5. Conclusions

Considering the existing water crisis that Cyprus is facing and the forecast for annual precipitation in the island, the need for development of new sustainable technologies such as seawater desalination is urgent. Furthermore, the integration of a desalination unit with a CSP system gives the opportunity for co-generation of electricity and heat, thus, the energy needed for desalination can be obtained through a renewable energy source.

In this paper, the experimental results for both a single effect and a MED unit were presented. The main conclusions from this work can be summarized as:

- A maximum performance ratio exists for each thermal input condition. This is where distillation unit performs the most efficiently, e.g. produces the maximum amount of distillate for a given amount of steam.
- Increasing the seawater reduces the amount of distillate produced; since more seawater mass is present and a larger fraction of the available thermal energy is devoted to sensible heating of the seawater.
- Decreasing the seawater reduces the amount of distillate produced; since less mass is available to completely wet the heat exchangers; dry spots occur reducing the overall heat transfer coefficient of the device and leading to a decrease in the amount of distillate produced.
- Increasing the temperature of the seawater feed increases the efficiency and the performance ratio of the device.
- Increasing the number of effects results in a higher *PR* value of the unit that is approximately increased by 0.7 every time that an effect is added to the system.
- Increasing the heating steam temperature decreases the thermal performance of the unit.
- The predictions of the control volume theoretical model developed overall are satisfactory. The model is unable to capture the maximum in the performance ratio since it cannot capture the physics of the dry out on the heat exchanger plates.

Further to this study, a four-effect distillation unit will be developed and evaluated in terms of the *PR*. Additionally; the control volume model will be expanded into a multiple-effect model in order to compare with the experimental results.

Acknowledgements

This work was supported by the STEP-EW project, which runs under the framework of Cross-border cooperation programme "Greece-Cyprus 2007–2013" and is co-financed by 80% by the European Commission (European Regional Development Fund) and by 20% by National Funds of Greece and Cyprus.

Nomenclature

Cp	—	specific heat capacity
m	—	mass flow rate
PR	—	performance ratio
Q	—	thermal load
T	—	temperature

U	—	heat transfer coefficient
X	—	salinity
λ	—	latent heat of vaporization

Subscripts

b	—	brine
cw	—	cooling water
d	—	distillate
e	—	evaporator
st	—	steam
sw	—	seawater
v	—	vapour
N	—	number of effects

References

[1] T. Zachariadis, Residential water scarcity in Cyprus: Impact of climate change and policy options, Water 2 (2010) 788–814.
[2] C. European, Water Scarcity and Droughts Report, Finland, 2006.
[3] P. Hadjinicolaou, C. Giannakopoulos, C. Zerefos, M.A. Lange, S. Pashiardis, J. Lelieveld, Mid-21st Century climate and weather extremes in Cyprus as projected by six regional climate models, Reg. Environ. Change 11 (2011) 441–457.
[4] T. Zachariadis, Climate change in Cyprus: Impacts and adaptation policies, Cyprus Econ. Policy Rev. 6 (2012) 21–37.
[5] IPCC, Renewable Energy Sources and Climate Change Mitigation, Cambridge University Press, Cambridge, 2011.
[6] M. Elimelech, W.A. Phillip, The future of seawater desalination: Energy, technology and the environment, Science 333 (2011) 712–717.
[7] V. Belessiotis, E. Delyannis, Water shortage and renewable energies (RE) desalination—Possible technological applications, Desalination 139 (2001) 133–138.
[8] C. Charcosset, A review of membrane processes and renewable energies for desalination, Desalination 245 (2009) 214–231.
[9] M. Al-Shammiri, M. Safar, Multi-effect distillation plants: State of the art, Desalination 126 (1999) 45–59.
[10] N.M. Wade, Distillation plant development and cost update, Desalination 136 (2001) 3–12.
[11] A. Vozar McKnight, M.D. Georgiou, M. Seong, J.G. Georgiadis, Analysis and design of a multi-effect desalination system with thermal vapor compression and harvested heat addition, Desalin. Water Treat. 31 (2011) 339–346.
[12] M. Darwish, Feed water arrangements in a multi-effect desalting system, Desalination 228 (2008) 30–54.
[13] S. Kalogirou, Economic analysis of a solar assisted desalination system, Renew. Energy 12 (1997) 351–367.
[14] J. Blanco, S. Malato, P. Fernández-Ibañez, D. Alarcón, W. Gernjak, M. Maldonado, Review of feasible solar energy applications to water processes, Renew. Sust. Energy Rev. 13 (2009) 1437–1445.
[15] A. Ghobeity, C.J. Noone, C.N. Papanicolas, A. Mitsos, Optimal time invariant operation of a power and water cogeneration solar-thermal plant, Sol. Energy 85 (9) (2011) 2295–2320.
[16] P. Palenzuela, G. Zaragoza, D. Alarcón, J. Blanco, Simulation and evaluation of the coupling of desalination units to parabolic-trough solar power plants in the Mediterranean region, Desalination 281 (2011) 379–387.
[17] C. Gomez-Camacho, L. Garcia-Rodriguez, Design parameter selection for a distillation system coupled to a solar parabolic through collector, Desalination 122 (1999) 195–204.
[18] Combined Solar Power and Desalination Plant: Techno-Economic Potential in Mediterranean Partner Countries, Report, 2010.
[19] J. Tonner, S. Hinge, C. Legorreta, Plates—The next breakthrough in thermal desalination, Desalination 134 (2001) 205–211.
[20] M. Georgiou, A. Bonanos, J. Georgiadis, Evaluation of a multiple-effect distillation unit under partial load operating conditions, Conf. Pap. Enegry 2013 (2013) 1–9.
[21] M.Z. Abedin, T. Tsuji, Y. Hattori, Direct numerical simulation for a time-developing natural-convection boundary layer along a vertical flat plate, Int. J. Heat Mass Transfer 52 (2009) 4525–4534.
[22] H.T. El-Dessouky, H.M. Ettouney, Single effect evaporation, in: Fundamentals of Salt Water Desalination, Elsevier, Amsterdam, 2002, pp. 20–44.
[23] M.H. Sharqawy, J.H. Lienhard V, S.M. Zubair, Thermophysical properties of seawater: A review of existing correlations and data, Desalin. Water Treat. 16 (2010) 354–380.
[24] H.T. El-Dessouky, H.M. Ettouney, F. Mandani, Performance of parallel feed multiple effect evaporation system for seawater desalination, Appl. Therm. Eng. 20 (2000) 1679–1706.
[25] F. Kafi, V. Renaudin, D. Alonso, J. Hornut, M. Weber, Experimental study of a three-effect plate evaporator: Seawater tests in La Spezia, Desalination 182 (2005) 175–186.